Photochemical & Photobiological Sciences

PAPER

Cite this: *Photochem. Photobiol. Sci.*, 2017, **16**, 220

Primary photophysical and photochemical processes for hexachloroosmate(IV) in aqueous solution

Evgeni M. Glebov,*[a,b] Ivan P. Pozdnyakov,[a,b] Svetlana G. Matveeva,[a] Alexei A. Melnikov,[c] Sergey V. Chekalin,[c] Marina V. Rogozina,[a,d] Vladislav V. Yudanov,[a,d] Vjacheslav P. Grivin[a] and Victor F. Plyusnin[a,b]

Received 20th October 2016,
Accepted 13th December 2016

DOI: 10.1039/c6pp00382f

rsc.li/pps

The photoaquation of the $Os^{IV}Cl_6^{2-}$ complex was studied by means of stationary photolysis, nanosecond laser flash photolysis and ultrafast kinetic spectroscopy. The $Os^{IV}Cl_5(OH)^{2-}$ complex was found to be the only reaction product. The quantum yield of photoaquation is rather low and wavelength-dependent. No impact of redox processes on photoaquation was revealed. The total characteristic lifetime of the process is about 80 ps. Three intermediates were recorded in the femto- and picosecond time domains and assigned to different Os(IV) species. The nature of intermediates and possible mechanisms of photoaquation are discussed.

1. Introduction

The ultrafast dynamics of transition metal complexes is an active area of research in chemical physics.[1–3] Primary photophysical processes are known in detail for only a few types of transition metal complexes. These include Cr(III) complexes,[4,5] polypyridyl complexes of Ru(II),[1,2,6] metal carbonyls,[1,7] and various complexes demonstrating spin crossover.[8,9]

Recently, we have reviewed the efforts in studying primary photophysical and photochemical processes for hexahalide complexes of tetravalent ions of platinum group metals (see ref. 10 and references therein). Five complexes of this type were the subjects of femtosecond studies, namely, $Pt^{IV}Cl_6^{2-}$, $Pt^{IV}Br_6^{2-}$, $Ir^{IV}Cl_6^{2-}$, $Ir^{IV}Br_6^{2-}$, and $Os^{IV}Br_6^{2-}$. Among them, the photophysics and photochemistry of $Pt^{IV}Br_6^{2-}$ in aqueous and alcoholic solutions were studied from absorption of a light quantum to the formation of final photolysis products.[11–13] For other mentioned complexes, the mechanisms are not as complete as for $Pt^{IV}Br_6^{2-}$.[10]

Complexes of osmium are potentially interesting in the field of photochemistry. The electronic configuration ($5d^6 6s^2$) of an osmium atom provides the existence of oxidation states from +8 to −2 (the most stable are the compounds with valences VIII, VI and IV),[14] which can provide a rich photochemistry. Nevertheless, studies on the photochemistry of osmium complexes, including such simple systems as Os(IV) hexahalide complexes are scarce. The main facts are as follows:

(1) It is known that the $Os^{IV}Br_6^{2-}$ complex in aqueous and methanol solutions undergoes photosolvation occurring in the picosecond time domain *via* the formation of the $^3Os^{IV}Br_5^-$ intermediate.[11,15] Additional data on the stationary and nanosecond laser flash photolysis of $Os^{IV}Br_6^{2-}$ are required to complete its photolysis mechanism.

(2) The $Os^{IV}Cl_6^{2-}$ complex effectively catalyzes the photodecomposition of chloroform in aerated solutions. The decomposition products are consistent with the mechanism in which the excited state of $Os^{IV}Cl_6^{2-}$ reduces chloroform, rather than photodissociation to an Os(III) complex and a chlorine atom.[16]

(3) Irradiation of hexahaloosmates(IV) in various polar solvents (water, acetonitrile, pyridine) results in solvation with the preferable formation of monosubstituted products.[17]

(4) The photochemistry of $Os^{IV}Cl_6^{2-}$ in aqueous and methanol solutions was studied in ref. 18 by means of stationary and nanosecond laser flash photolysis. Because this complex is the subject of the current work, we present a brief summary of conclusions:[18]

(a) The near UV irradiation of $Os^{IV}Cl_6^{2-}$ in aqueous and methanolic solutions resulted in successive photosolvation with the formation of $Os^{IV}Cl_5(H_2O)^-$ and $Os^{IV}Cl_5(CH_3OH)^-$

[a]*Voevodsky Institute of Chemical Kinetics and Combustion, 3 Institutskaya Str., 630090 Novosibirsk, Russian Federation. E-mail: glebov@kinetics.nsc.ru; Fax: +7 383 3307350; Tel: +7 383 3309150*
[b]*Novosibirsk State University, 2 Pirogova Str., 630090 Novosibirsk, Russian Federation*
[c]*Institute of Spectroscopy, Russian Academy of Sciences, 5 Fizicheskaya Str., 119333 Troitsk, Moscow, Russian Federation. E-mail: melnikov@isan.troitsk.ru*
[d]*Vologograd State University, 100 University Ave., 400062 Volgograd, Russian Federation. E-mail: rogozina@volsu.ru*

complexes in the first stage. No effect of dissolved oxygen was observed.

(b) The characteristic time of photosolvation was less than 50 ns; no intermediates were recorded in the laser flash photolysis experiments. Therefore, photosolvation occurs *via* heterolytic cleavage of the Os–Cl bond; no redox reactions are involved.

(c) The near UV irradiation of the $Os^{IV}Cl_5(H_2O)^-$ complex resulted in further aquation independent of the presence of dissolved oxygen.

(d) The near UV irradiation of the $Os^{IV}Cl_5(CH_3OH)^-$ complex in deaerated solutions resulted in the reduction of Os(IV) to Os(III). Electron transfer from a solvent molecule to the light-excited complex was proposed as a primary photochemical process.

Continuing our efforts in studying primary light-induced processes for hexahalide complexes of platinum metals,[10] in this work we present the results on the ultrafast kinetic spectroscopy of $Os^{IV}Cl_6^{2-}$ in aqueous solutions.

2. Experimental

Solutions of the $OsCl_6^{2-}$ complex were prepared from $Na_2OsCl_6{\cdot}H_2O$ salt (Aldrich). Deionized water was used for sample preparation. If necessary, pH of the solutions was changed by addition of a pre-calculated amount of perchloric acid. The pH value was controlled by the ion-meter ANION-4100 (LTD Infraspak-Analit, Russia) with the combined electrode ESK-10614. When necessary, the samples were deaerated by bubbling with argon.

UV absorption spectra were recorded using a Varian Cary 50 (Varian Inc.) spectrophotometer. Stationary photolysis was performed using the irradiation of a high-pressure mercury lamp with a set of glass filters for separating necessary wavelengths. In several experiments, the excimer XeCl lamp (excilamp) was used as a quasicontinuous source of UV-irradiation at 308 nm (half width of light pulse, 5 nm; pulse duration, 1 μs; frequency, 200 kHz; incident light flux, 8×10^{15} photons per cm^2 per s).[19] A light power meter SOLO 2 (Gentec, Canada) was used to measure the radiation intensity for the quantum yield calculations.

Nanosecond laser flash photolysis experiments were performed using excitation by irradiation of a Nd:YAG laser (Lotis TII, Belarus, 355 nm, 5 ns pulse duration, up to 10 mJ per pulse energy). The setup is described in detail in ref. 20.

Pump–probe spectroscopy was used to study transient absorption of the samples in the picosecond time domain. The experimental setup is described in detail in ref. 21. The samples were excited by ~60 fs pulses (energy *ca.* 1 μJ, pulse repetition rate 1 kHz) at ~400 nm (second harmonic of a Ti:sapphire generator-amplifier system, CDP Ltd, Moscow, Russia). 200 pulses were used to record a single time-resolved spectrum. Each kinetic curve contained 110 points (60 points with a 100 fs step, 20 points with a 500 fs step, and 30 points with a 3 ps step). The investigated solutions (total volume of 20 ml) were pumped through a 1 mm quartz cell at room temperature to provide uniform irradiation and avoid possible degradation due to photochemical reactions. The ExciPro program (CDP System Corporation) was used for corrections of the group velocity dispersion. The corrected experimental data were further globally fitted using a three-exponential model.

3. Results and discussion

3.1. Spectroscopy of $Os^{IV}Cl_6^{2-}$

$Os^{IV}Cl_6^{2-}$ is a low spin complex with the $5d^4$ electronic configuration. To clarify the further description, the approximate structure of the orbitals based on the results of Jørgensen[22,23] is shown in Fig. 1. In the framework of a simple crystal field approach with the O_h symmetry its ground state is triplet ($^3T_{1g}$).[24] In the literature, the octahedral symmetry is typically used in studies on $Os^{IV}Cl_6^{2-}$ spectroscopy[22,24] in spite of the Jahn–Teller distortion to lower the symmetry.

The UV spectrum of $Os^{IV}Cl_6^{2-}$ in aqueous solutions (curve 1 in Fig. 2) was studied in ref. 22, 23, 25 and 26. The values of molar absorption coefficients reported in different studies are not completely coincident. The quantitative data obtained in this work are close to those reported by Jørgensen[22] and sufficiently different from the data obtained by Blasius and Preetz.[25] Note that Broszkiewicz[26] gave the ratios of band intensities different from all the other studies. We report here the values of the molar absorption coefficients for $Os^{IV}Cl_6^{2-}$ in

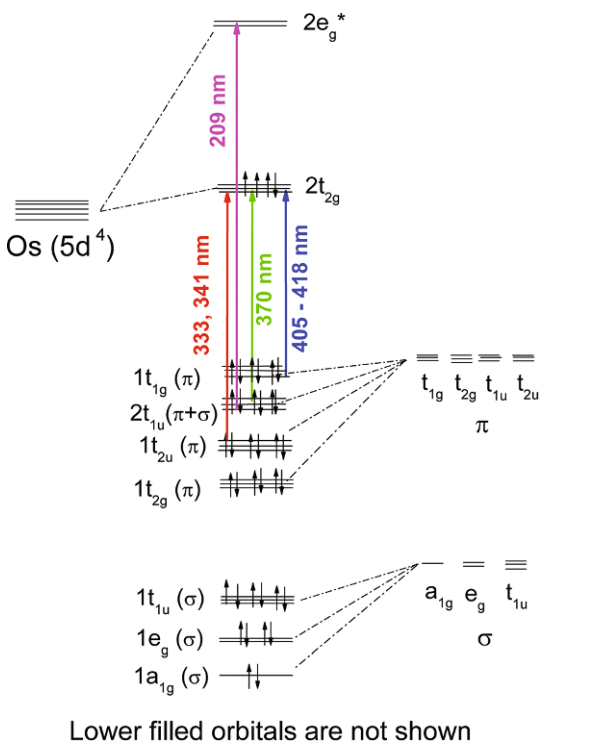

Fig. 1 The approximate structure of the molecular orbitals of the $OsCl_6^{2-}$ complex according to ref. 22 (non-relativistic approximation). Arrows correspond to the LMCT transitions.

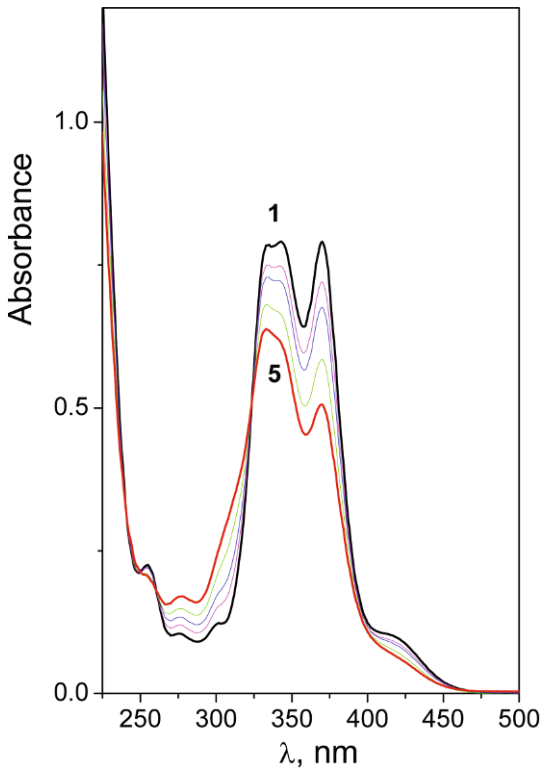

Fig. 2 Changes in the UV absorption spectrum caused by irradiation (405 nm, 1 cm quartz cell) of $Os^{IV}Cl_6^{2-}$ in aqueous solution; initial concentration 1.0×10^{-4} M, initial pH 7.8. Curves 1–5 correspond to 0, 50, 85, 177 and 297 min of irradiation, respectively.

aqueous solutions (pH ~ 7); the results are close to those of Jørgensen.[22]

The interpretation of the absorption bands of the initial complex in the framework of the octahedral symmetry is presented in Fig. 1. A low intense band that appeared as a shoulder in the region of 405–418 nm (molar absorption coefficient $\varepsilon \sim 900$ M^{-1} cm^{-1}) was assigned to an LMCT transition. According to Jørgensen's interpretation[22,23] this band corresponds to the $\pi_{Cl}(t_{1g}) \rightarrow Os(t_{2g})$ promotion (Fig. 1). The LMCT bands in the region of 320–375 nm are represented by a doublet (λ_{max} = 335 and 342 nm, ε = 7850 and 7900 M^{-1} cm^{-1} correspondingly) and a single band with a maximum at 370 nm, ε = 7900 M^{-1} cm^{-1}. These bands correspond to $\pi_{Cl}(t_{2u}) \rightarrow Os(t_{2g})$ and $(\pi + \sigma)_{Cl}(t_{1u}) \rightarrow Os(t_{2g})$ promotions.[22] The most intense LMCT band with the maximum at 209 nm (ε = 18 500 M^{-1} cm^{-1}) was assigned to the $\pi_{Cl} \rightarrow Os(e_g)$ promotion.[22] Bands with the maxima at 301, 278, and 255 nm ($\varepsilon \sim$ 1000, 700 and 2000 M^{-1} cm^{-1} correspondingly[22]) are caused by the d–d transitions; they are partially superimposed with the LMCT bands.

3.2. Photochemistry of the $Os^{IV}Cl_6^{2-}$ complex in aqueous solutions

The slow reversible thermal aquation of $Os^{IV}Cl_6^{2-}$ was observed in accord with ref. 27. The equilibrium at room temperature is established with the characteristic time of ~24 h. The impact of the thermal reaction was taken into account when the quantum yield of photoaquation was estimated.

Changes in the UV absorption spectrum caused by 405 nm irradiation are shown in Fig. 2. Four isosbestic points at 240, 250, 261 and 324 nm were conserved. Therefore, only one photochemical process takes place. Based on the results,[17] one can conclude that this process is photoaquation. No effect of dissolved oxygen on photolysis was found. Prolonged irradiation results in further photoaquation.[18]

The irradiation results in an increase of solution acidity (Fig. 3). It means that the primary product of aquation, the $Os^{IV}Cl_5(H_2O)^-$ complex, possesses acidic properties. In fact, the product of photoaquation in solutions with an initially neutral pH is the hydroxocomplex $Os^{IV}Cl_5(OH)^{2-}$ (eqn (1)), but not the $Os^{IV}Cl_5(H_2O)^-$ complex, as proposed in ref. 18.

$$Os^{IV}Cl_6^{2-} + H_2O \xrightarrow{h\nu} Os^{IV}Cl_5(OH)^{2-} + Cl^- + H^+ \quad (1)$$

Miano and Garner[27] have reported the UV spectrum of $OsCl_5(H_2O)^-$, which has the band with the maximum at 344 nm (ε = 7200 M^{-1} cm^{-1} in 2.5 F $HClO_4$). In order to examine the difference in the UV spectra of the $Os^{IV}Cl_5(OH)^{2-}$ and $Os^{IV}Cl_5(H_2O)^-$ complexes we performed the experiment on the stationary photolysis of $Os^{IV}Cl_6^{2-}$ followed by acidification. The result is shown in Fig. 4. The initial solution of $Os^{IV}Cl_6^{2-}$ with a pH close to neutral (curve 1) was irradiated to pH 4.5,

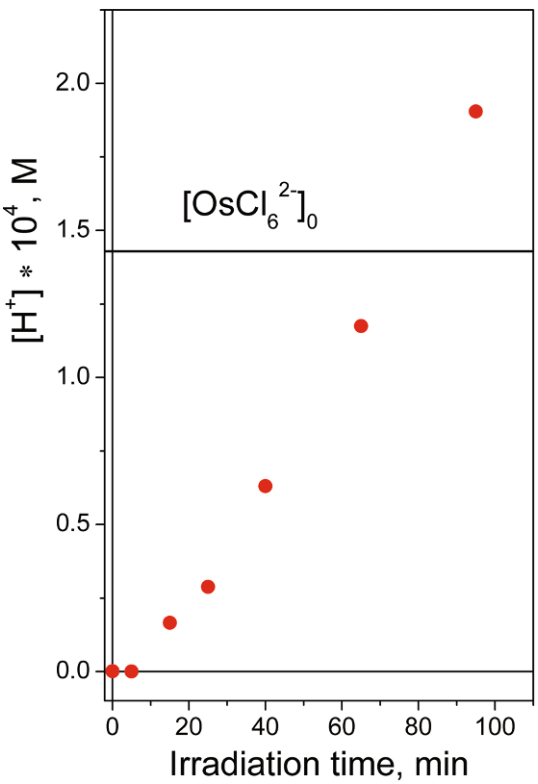

Fig. 3 Changes in the acidity of solution in the course of $OsCl_6^{2-}$ photolysis (308 nm, initial concentration 1.43×10^{-4} M).

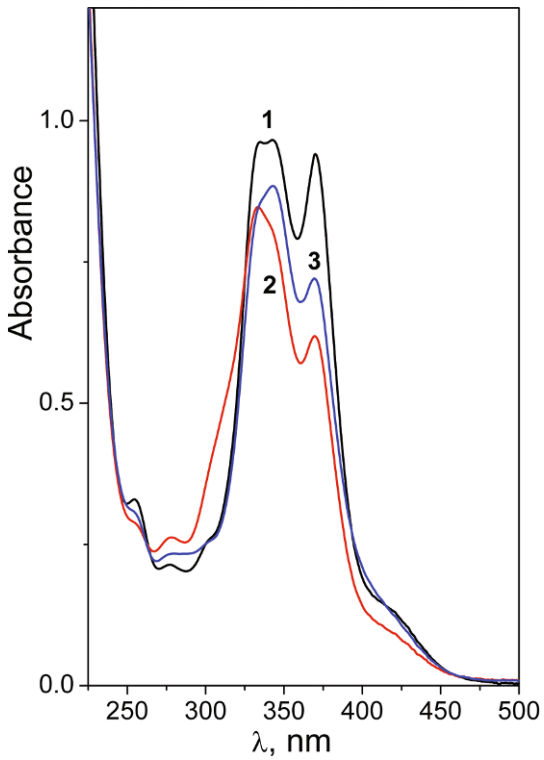

Fig. 4 Changes in the UV spectrum of aqueous $OsCl_6^{2-}$ (curve 1, 1.22×10^{-4} M in a 1 cm cell, initial pH 6.8) caused by 37 min of irradiation at 308 nm (curve 2, pH 4.5) and acidification to pH 1.5 (curve 3).

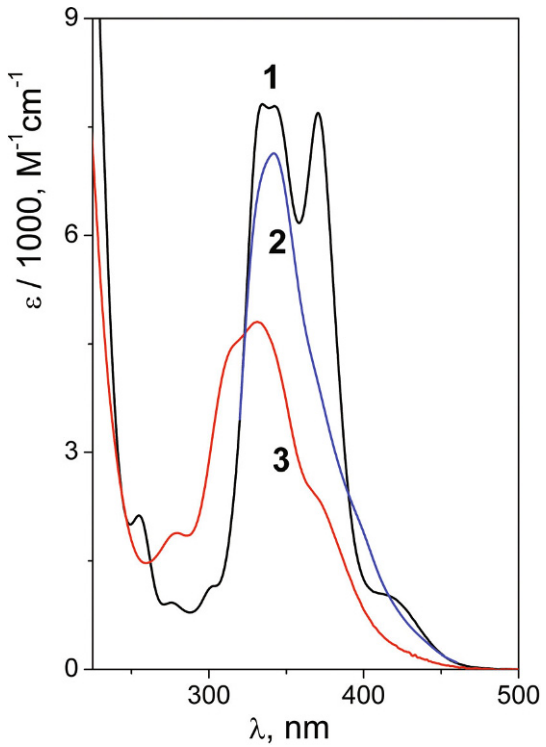

Fig. 5 UV spectra of aqueous $Os^{IV}Cl_6^{2-}$ (curve 1), $Os^{IV}Cl_5(H_2O)^-$ (curve 2); adopted from ref. 27, and $Os^{IV}Cl_5(OH)^{2-}$ (curve 3, see text).

when isosbestic points were still conserved (the spectrum of the irradiated solution is shown by curve 2). Then the solution was acidified to pH 1.5 (curve 3). Further acidification did not result in changes in the UV spectrum testifying that all the $Os^{IV}Cl_5(OH)^{2-}$ complexes transited to $Os^{IV}Cl_5(H_2O)^-$. One can see in Fig. 4 that the difference in the spectra of the $Os^{IV}Cl_5(OH)^{2-}$ and $Os^{IV}Cl_5(H_2O)^-$ complexes is sufficient.

The conservation of isosbestic points (Fig. 2) and changes in the pH of the irradiated solutions allowed us to restore the spectrum of the $Os^{IV}Cl_5(OH)^{2-}$ hydroxocomplex. Its spectrum was calculated from the spectral changes in the course of photolysis in assumption that the concentration of $Os^{IV}Cl_5(OH)^{2-}$ is equal to the concentration of the released H^+ (eqn (1)). The result is shown in Fig. 5 (curve 3). For reference, the spectrum of the $Os^{IV}Cl_5(H_2O)^-$ complex adopted from ref. 27 is shown (curve 2). As one can expect from Fig. 4, the spectra of $Os^{IV}Cl_5(OH)^{2-}$ and $Os^{IV}Cl_5(H_2O)^-$ are rather different.

Using the spectrum $Os^{IV}Cl_5(OH)^{2-}$, we determined the quantum yield of reaction (1). The results are shown in Table 1. One can see that the quantum yield is rather low and wavelength-dependent. For the low-energy LMCT band corresponding to $\pi_{Cl} \rightarrow t_{2g}$ promotion, the quantum yield of photoaquation is less than 1%. This is similar to the case of the $IrCl_6^{2-}$ complex, for which the low-energy LMCT bands in the visible spectral range are photochemically inert, while the near UV LMCT bands superimposed with the d–d bands demonstrate moderate photochemical activity.[28,29]

Table 1 Quantum yields of $OsCl_6^{2-}$ photoaquation

$\varphi^{313\ nm}$	$\varphi^{405\ nm}$
$(3.0 \pm 0.8) \times 10^{-2}$	$(5 \pm 1) \times 10^{-3}$
2.3×10^{-2} [a]	

[a] Measured in ref. 18 (with the correction to the differences in the molar absorption coefficients of the initial complex and the product).

Experiments on the nanosecond laser flash photolysis of $Os^{IV}Cl_6^{2-}$ in aqueous solutions demonstrated only instant changes in the absorption spectrum (in accord with earlier experiments mentioned in ref. 18). The characteristic kinetic curves are shown in Fig. 6. No effect of dissolved oxygen on the kinetic curves was found.

Because of low quantum yields, the signals are rather small. The characteristic time of photosolvation was less than 50 ns (*i.e.* time resolution of the experimental setup); no intermediates (which could be either Os(III) or Os(V) complexes; the latter were observed by Broszkiewicz by means of pulse radiolysis[26]) were recorded. The sign of the differential changes in absorption (Fig. 6) corresponds to the difference in the absorption of aquated and initial complexes obtained in stationary experiments (Fig. 2). One can see an instant increase in absorption at 320 nm and an instant decrease at 380 nm in accord with the positions of the isosbestic points in the stationary experiment (Fig. 2).

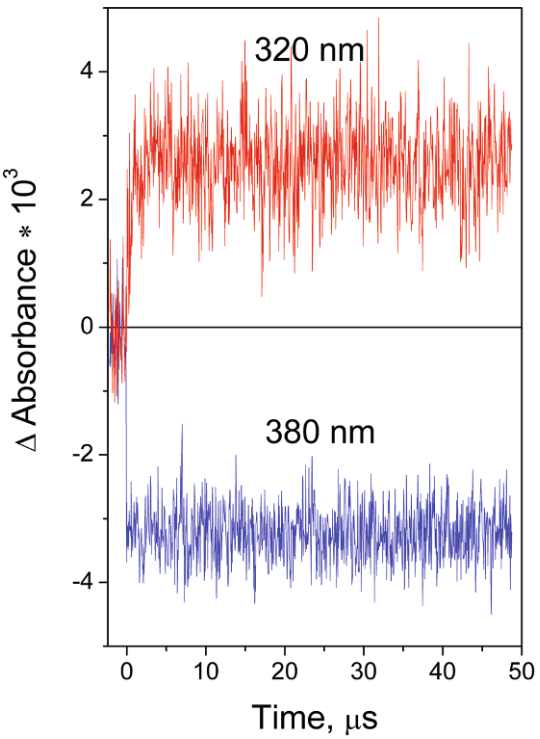

Fig. 6 Laser flash photolysis (355 nm, initial concentration 7.8×10^{-5} M, air-saturated solution) of $OsCl_6^{2-}$ in water. Examples of kinetic curves.

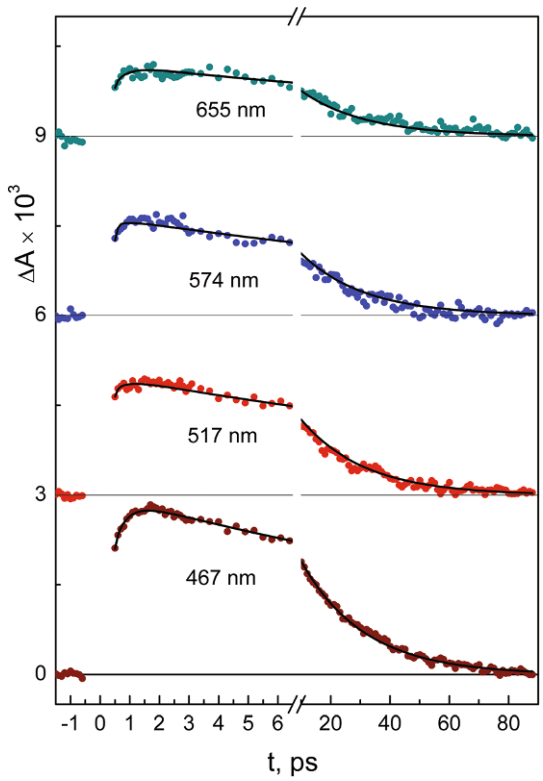

Fig. 7 Results of ultrafast kinetic spectroscopy experiments (λ_{pump} = 400 nm) with $Os^{IV}Cl_6^{2-}$ (2.3×10^{-4} M) in aqueous solution. Experimental kinetic curves (dots) and the best three-exponential global fits (solid lines).

Therefore, we can conclude (as it has been stated in ref. 18) that photoaquation occurs *via* the heterolytic cleavage of the Os–Cl bond; no redox reactions are involved.

3.3. Ultrafast kinetic spectroscopy of $Os^{IV}Cl_6^{2-}$

Experiments on the ultrafast kinetic spectroscopy were performed with excitation in the region of 400 nm corresponding to the intersection of two absorption bands. In the framework of the octahedral geometry, one of these bands is the long-wavelength wing of the intense $(\pi + \sigma)_{Cl}(t_{1u}) \rightarrow Os(t_{2g})$ transition, and the second band corresponds to the less intense $\pi_{Cl}(t_{1g}) \rightarrow Os(t_{2g})$ transition (Fig. 1). Both transitions are spin-allowed, therefore the immediately forming Franck–Condon (FC) state, in spite of the transition type, is a spin triplet. Further we will mark this FC state as ^{3}(LMCT). Because of low quantum yields of photochemical reactions in this wavelength region (Table 1), we in fact examine the photophysical processes which resulted in the recovery of the initial complex ground state.

In the course of ultrafast kinetic spectroscopy experiments the intermediate absorption spectra were recorded in the wavelength range of 440–680 nm. The characteristic kinetic curves are shown in Fig. 7. One can see that the experimental points corresponding to time delays falling into the interval (−500 fs) $< \tau >$ (300 fs) are omitted because they are affected by the coherent artifact caused by the coherent interactions between pump and probe pulses.[30] One can observe a partial increase in the intermediate absorption with the characteristic time *ca.* 1 ps and its complete disappearance within the 80 ps time interval.

The kinetic curves obtained in the experiments on the ultrafast pump–probe spectroscopy were globally fitted using a triexponential function (2) (the biexponential fit did not give a satisfactory description).

$$\Delta A(\lambda, t) = A_1(\lambda)e^{-k_1 t} + A_2(\lambda)e^{-k_2 t} + A_3(\lambda)e^{-k_3 t} \quad (2)$$

When the kinetic curves are fitted using the triexponential function (2), the sequential decay of the transient absorption A → B → C → (ground state + products) is proposed. The species associated difference spectra (SADS) of the individual components were calculated by means of the formulae derived in ref. 31. The SADS corresponding to the kinetic curves are shown in Fig. 8. The time constants extracted by using the global fit procedure are collected in Table 2.

$$S_A(\lambda) = A_1(\lambda) + A_2(\lambda) + A_3(\lambda) \quad (3)$$

$$S_B(\lambda) = A_2(\lambda)\frac{k_1 - k_2}{k_1} + A_3(\lambda)\frac{k_1 - k_3}{k_1} \quad (4)$$

$$S_C(\lambda) = A_3(\lambda)\frac{(k_1 - k_3)(k_2 - k_3)}{k_1 k_2} \quad (5)$$

After excitation the transient absorption spectrum appears as a wide band covering all the regions of observation

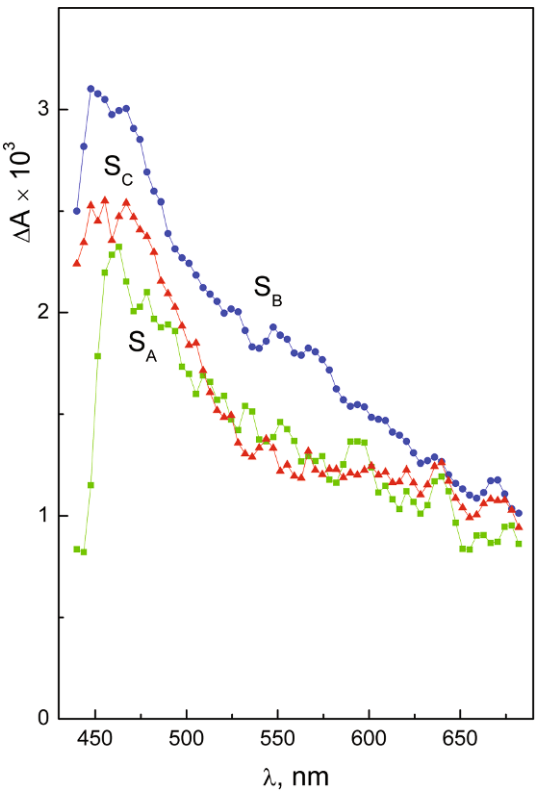

Fig. 8 Results of the ultrafast kinetic spectroscopy experiment (λ_{pump} = 400 nm) with $Os^{IV}Cl_6^{2-}$ (2.3 × 10^{-4} M) in aqueous solution. Species associated difference spectra (SADS) obtained from the three-exponential global fit (eqn (2)) of experimental kinetic curves and formulae (3)–(5).

Table 2 Ultrafast kinetic spectroscopy (excitation at 400 nm) of $Os^{IV}Cl_6^{2-}$ in aqueous solutions. Characteristic lifetimes. FC – Franck–Condon state, KI – key intermediate, GS – ground state

τ_1, fs	Process	τ_2, ps	Process	τ_3, ps	Process
330 ± 160	FC → (KI)*	3.0 ± 1.8	(KI)* → KI	23 ± 3	KI → GS + products

(440–680 nm, SADS S_A in Fig. 8). The maximum of this band lies at 460 nm. Then the differential absorption increases (SADS S_B in Fig. 6; this increase is the most prominent at shorter wavelengths). The second observed process is the narrowing of the absorption band resulting in the formation of SADS S_C (Fig. 8). The last process results in the complete disappearance of the intermediate absorption (see the kinetic curves in Fig. 7).

The interpretation of the observed spectral changes (Table 2) is as follows. In the ideal case (if no coherent artifact exists), the initial SADS S_A corresponds to the differential spectrum of the FC state, and the first observed process with the characteristic time of 300–400 fs corresponds to the transition from the FC state to the key intermediate (KI), whose spectrum is represented by the SADS S_B. The KI could be the lowest electronic excited state of the initial complex or a pentacoordinated intermediate of Os(IV) (this point is discussed below). This intermediate is vibrationally hot. The second observed process with the characteristic time of several picoseconds is the vibrational cooling of the KI, probably superimposed with the translational solvent relaxation. The resulted relaxed state is represented by the SADS S_C. The final process with the characteristic lifetime of several tens of picoseconds is the transition of the relaxed KI to the $Os^{IV}Cl_6^{2-}$ ground state and to the reaction product, which is the aquated $Os^{IV}Cl_5(H_2O)^-$ complex (its formation is followed by acid dissociation). The impact of the reactive channel of the KI transformation is small (see Table 1). The absence of the residual absorption in the picosecond time domain is in agreement with the absence of the intermediate absorption observed in the nanosecond laser flash photolysis experiments.

The described ideal picture is affected by the coherent artifact. Because of the artifact, it is not possible to extract precisely the SADS of the Franck–Condon state and the lifetime of its transformation from the experimental data (initial parts of kinetics in Fig. 7). In fact, the SADS S_A is a superposition of the differential spectra of the Franck–Condon state and the KI, and the first extracted lifetime (τ_1) in Table 2 is an estimation of the real characteristic time of the first process.

Based on the observed experimental data and literature analogues, two tentative mechanisms of ultrafast processes for $Os^{IV}Cl_6^{2-}$ could be put forward. These mechanisms are different in the nature of the KI species. In the framework of the first mechanism described by eqn. (6)–(10), the initially formed excited state ^{3}(LMCT) is followed by the intercombination conversion, and the key intermediate is the lowest electronic excited state of the initial complex, as it occurs for the case of $Ir^{IV}Cl_6^{2-}$.[32,33] According to ref. 24, this is the $^1T_{2g}$ state, which is vibrationally hot. The second observed process is the vibrational cooling of the hot $^1T_{2g}$ state. The last process is the transition of $OsCl_6^{2-}(^1T_{2g})$ to the ground state and (with a low probability) to the photoaquation product.

3.4 Mechanism 1

$$Os^{IV}Cl_6^{2-}(^3T_{1g}) \xrightarrow{h\nu} {}^3(LMCT)_{hot} \quad (6)$$

$$^3(LMCT)_{hot} \rightarrow Os^{IV}Cl_6^{2-}\left(^1T_{2g}^*\right)_{hot} \quad (7)$$

$$Os^{IV}Cl_6^{2-}\left(^1T_{2g}^*\right)_{hot} \rightarrow Os^{IV}Cl_6^{2-}\left(^1T_{2g}^*\right) \quad (8)$$

$$Os^{IV}Cl_6^{2-}\left(^1T_{2g}^*\right) \rightarrow Os^{IV}Cl_6^{2-}(^3T_{1g}) \quad (9)$$

$$Os^{IV}Cl_6^{2-}\left(^1T_{2g}^*\right) \xrightarrow{H_2O} Os^{IV}Cl_5(H_2O)^{2-} + Cl^- \quad (10)$$

It should be noted that Mechanism 1 does not explain the wavelength dependence of the photoaquation quantum yield (Table 1). To explain this dependence, one has to propose that

the excitation at the shorter wavelength opens a new reactive channel, and the reaction proceeds from the excited state different from $^1T_{2g}$.

The second mechanism is similar to that reported for the $Os^{IV}Br_6^{2-}$ complex.[11,15] One can assume that the ^{3}(LMCT) excited state of $Os^{IV}Cl_6^{2-}$ is quickly depopulated to the lowest excited state, which is dissociative. In the framework of this mechanism, KI is the pentacoordinated complex of Os(IV), which is still situated in the solvent cage with the Cl^- anion. For the case of $Os^{IV}Br_6^{2-}$ photolysis, it was shown that the triplet state of the pentacoordinated complex is thermodynamically more stable than the singlet one.[11,15] One can assume that the same relation is fulfilled for the $^3Os^{IV}Cl_5^-$ and $^1Os^{IV}Cl_5^-$ species. In this case, we can write a tentative Mechanism 2 (eqn (11)–(14)).

3.5 Mechanism 2

$$^3(\mathrm{LMCT})_{\mathrm{hot}} \rightarrow \{Os^{IV}Cl_5^- \cdots Cl^-\}^{\mathrm{cage}}_{\mathrm{hot}} \quad (11)$$

$$^3\{Os^{IV}Cl_5^- \cdots Cl^-\}^{\mathrm{cage}}_{\mathrm{hot}} \rightarrow \{Os^{IV}Cl_5^- \cdots Cl^-\}^{\mathrm{cage}} \quad (12)$$

$$^3\{Os^{IV}Cl_5^- \cdots Cl^-\}^{\mathrm{cage}} \rightarrow Os^{IV}Cl_6^{2-}(^3T_{1g}) \quad (13)$$

$$^3\{Os^{IV}Cl_5^- \cdots Cl^-\}^{\mathrm{cage}} \xrightarrow{H_2O} Os^{IV}Cl_5(H_2O)^- + Cl^- \quad (14)$$

Reaction (11) represents the result of the first experimentally observed process (which is partially hindered by the coherent artifact). The initially formed ^{3}(LMCT) state is dissociative resulting in the formation of the $\{^3Os^{IV}Cl_5^-\cdots Cl^-\}^{cage}$ pair. Note that the increase in the excitation energy can result in the increase of the relative kinetic energy of the escaping Cl^- anion, which can provide a tentative explanation of the wavelength dependence of the quantum yield of photosolvation (Table 1).

The second observed reaction (12) is the vibrational cooling of the KI ($^3Os^{IV}Cl_5^-$, as proposed). The last observed process represented by reactions (13) and (14) is the recovery of the ionic pair to the ground state of $Os^{IV}Cl_6^{2-}$ and (with a very low probability) the formation of the reaction product.

4. Conclusions

In this work we examined the primary photochemical processes for the $Os^{IV}Cl_6^{2-}$ complex in aqueous solutions. The resulting process is photoaquation with the formation of the $Os^{IV}Cl_5(OH)^{2-}$ hydroxocomplex. The total time of the process was found to be about 80 ps; no influence of redox processes was revealed. Based on the experimental data, two possible reaction mechanisms were proposed. The difference between these mechanisms is in the nature of the Os(IV) intermediates. To make a choice between the two mechanisms, additional studies are in progress.

Acknowledgements

Financial support from the Russian Science Foundation (Grant No. 15-13-10012) is gratefully acknowledged.

Notes and references

1 A. Vlcek Jr., *Coord. Chem. Rev.*, 2000, **200–202**, 933.
2 J. K. McCusker, *Acc. Chem. Res.*, 2003, **36**, 876.
3 L. S. Forster, *Coord. Chem. Rev.*, 2006, **250**, 2023.
4 E. A. Juban, A. L. Smeigh, J. E. Monat and J. K. McCusker, *Coord. Chem. Rev.*, 2006, **250**, 1783.
5 J. N. Schrauben, K. L. Dillman, W. F. Beck and J. K. McCusker, *Chem. Sci.*, 2010, **1**, 405.
6 R. Compton, H. K. Gerardi, D. Weidinger, D. J. Brown, W. J. Dressick, E. J. Heilweil and J. C. Owrutsky, *Chem. Phys.*, 2013, **422**, 135.
7 J. P. Lomont, S. C. Nguyen and C. B. Harris, *Acc. Chem. Res.*, 2014, **47**, 1634.
8 A. Marino, P. Chakraborty, M. Servol, M. Lorenc, E. Collet and A. Hauser, *Angew. Chem., Int. Ed.*, 2014, **53**, 3863.
9 C. Sousa, C. de Graaf, A. Rudavskyi, R. Broer, J. Tatchen, M. Etinski and C. M. Marian, *Chem. – Eur. J.*, 2013, **19**, 17541.
10 E. M. Glebov, I. P. Pozdnyakov, V. F. Plyusnin and I. Khmelinskii, *J. Photochem. Photobiol., C*, 2015, **24**, 1.
11 I. L. Zheldakov, M. N. Ryazantsev and A. N. Tarnovsky, *J. Phys. Chem. Lett.*, 2011, **2**, 1540.
12 E. M. Glebov, A. V. Kolomeets, I. P. Pozdnyakov, V. F. Plyusnin, V. P. Grivin, N. V. Tkachenko and H. Lemmetyinen, *RSC Adv.*, 2012, **2**, 5768.
13 E. M. Glebov, A. V. Kolomeets, I. P. Pozdnyakov, V. P. Grivin, V. F. Plyusnin, N. V. Tkachenko and H. Lemmetyinen, *Russ. Chem. Bull, Int. Ed.*, 2013, **62**, 1540.
14 P. A. Lay and W. D. Harman, Adv. Inorg. Chem., in *Recent Advances in Osmium Chemistry*, ed. A. G. Sykes, Academic Press, Inc., Sad Diego, California, 1991, vol. 37, pp. 219–380.
15 I. L. Zheldakov, *Ultrafast Photophysics and Photochemistry of Hexacoordinated Bromides of Pt(IV), Os(IV), and Ir(IV) in the Condensed Phase Studied by Femtosecond Pump-Probe Spectroscopy*, Ph. D. Thesis, Bowling Green State University, 2010.
16 L. A. Pena and P. E. Hoggard, *Photochem. Photobiol.*, 2010, **86**, 467.
17 Von W. Casenpusch and W. Preetz, *Z. Anorg. Allg. Chem.*, 1977, **432**, 107.
18 E. M. Glebov, V. F. Plyusnin, V. P. Grivin and Yu. V. Ivanov, *Russ. J. Coord. Chem.*, 1997, **23**, 580.
19 E. Sosnin, T. Oppenlander and V. Tarasenko, *J. Photochem. Photobiol., C*, 2006, **7**, 145.
20 I. P. Pozdnyakov, V. F. Plyusnin, V. P. Grivin, D. Yu. Vorobyev, N. M. Bazhin and E. Vauthey, *J. Photochem. Photobiol., A*, 2006, **182**, 75–81.
21 S. V. Chekalin, *Phys. Usp.*, 2006, **49**, 634.

22 C. K. Jørgensen, *Mol. Phys.*, 1959, **2**, 309.
23 C. K. Jørgensen and W. Preetz, *Z. Naturforsch.*, 1967, **22a**, 945.
24 S. M. Khan, H. H. Patterson and H. Engstrom, *Mol. Phys.*, 1978, **35**, 1623.
25 E. Blasius and W. Z. Preetz, *Z. Anorg. Allg. Chem.*, 1965, **335**, 16.
26 R. K. Broszkiewicz, *Radiat. Phys. Chem.*, 1977, **10**, 303.
27 R. R. Miano and C. S. Garner, *Inorg. Chem.*, 1965, **4**, 337.
28 L. Moggi, G. Varani, M. F. Manfrin and V. Balzani, *Inorg. Chim. Acta*, 1970, **4**, 335.
29 E. M. Glebov, V. F. Plyusnin, N. V. Tkachenko and H. Lemmetyinen, *Chem. Phys.*, 2000, **257**, 79.
30 L. Palfrey and T. F. Heinz, *J. Opt. Soc. Am. B*, 1985, **2**, 674.
31 A. S. Rury and R. J. Sension, *Chem. Phys.*, 2013, **422**, 220.
32 E. M. Glebov, A. V. Kolomeets, I. P. Pozdnyakov, V. F. Plyusnin, N. V. Tkachenko and H. Lemmetyinen, *Photochem. Photobiol. Sci.*, 2011, **10**, 1709.
33 E. M. Glebov, I. P. Pozdnyakov, A. A. Melnikov and S. V. Chekalin, *J. Photochem. Photobiol., A*, 2014, **292**, 34.